Research Article | Vol. 25, No. 14 | 10 Jul 2017 | OPTICS EXPRESS 16282
Optics EXPRESS

Terahertz quantum-cascade lasers as high-power and wideband, gapless sources for spectroscopy

Benjamin Röben,* Xiang Lü, Martin Hempel, Klaus Biermann, Lutz Schrottke, and Holger T. Grahn

Paul-Drude-Institut für Festkörperelektronik, Leibniz-Institut im Forschungsverbund Berlin e. V., Hausvogteiplatz 5–7, 10117 Berlin, Germany
roeben@pdi-berlin.de

Abstract: Terahertz (THz) quantum-cascade lasers (QCLs) are powerful radiation sources for high-resolution and high-sensitivity spectroscopy with a discrete spectrum between 2 and 5 THz as well as a continuous coverage of several GHz. However, for many applications, a radiation source with a continuous coverage of a substantially larger frequency range is required. We employed a multi-mode THz QCL operated with a fast ramped injection current, which leads to a collective tuning of equally-spaced Fabry-Pérot laser modes exceeding their separation. A continuous coverage over 72 GHz at about 4.7 THz was achieved. We demonstrate that the QCL is superior to conventional sources used in Fourier transform infrared spectroscopy in terms of the signal-to-noise ratio as well as the dynamic range by one to two orders of magnitude. Our results pave the way for versatile THz spectroscopic systems with unprecedented resolution and sensitivity across a wide frequency range.

OCIS codes: (140.3070) Infrared and far-infrared lasers; (140.3600) Lasers, tunable; (140.5965) Semiconductor lasers, quantum cascade; (300.6270) Spectroscopy, far infrared; (300.6320) Spectroscopy, high-resolution; (300.6495) Spectroscopy, terahertz

References and links

1. H.-W. Hübers, S. G. Pavlov, H. Richter, A. D. Semenov, L. Mahler, A. Tredicucci, H. E. Beere, and D. A. Ritchie, "High-resolution gas phase spectroscopy with a distributed feedback terahertz quantum cascade laser," Appl. Phys. Lett. **89**, 061115 (2006).
2. L. Consolino, S. Bartalini, H. E. Beere, D. A. Ritchie, M. S. Vitiello, and P. De Natale, "THz QCL-based cryogen-free spectrometer for in situ trace gas sensing," Sensors **13**, 3331–3340 (2013).
3. T. Hagelschuer, N. Rothbart, H. Richter, M. Wienold, L. Schrottke, H. T. Grahn, and H.-W. Hübers, "High-spectral-resolution terahertz imaging with a quantum-cascade laser," Opt. Express **24**, 13839–13849 (2016).
4. Y. Ren, J. N. Hovenier, R. Higgins, J. R. Gao, T. M. Klapwijk, S. C. Shi, A. Bell, B. Klein, B. S. Williams, S. Kumar, Q. Hu, and J. L. Reno, "Terahertz heterodyne spectrometer using a quantum cascade laser," Appl. Phys. Lett. **97**, 161105 (2010).
5. L. Schrottke, M. Wienold, R. Sharma, X. Lü, K. Biermann, R. Hey, A. Tahraoui, H. Richter, H.-W. Hübers, and H. T. Grahn, "Quantum-cascade lasers as local oscillators for heterodyne spectrometers in the spectral range around 4.745 THz," Semicond. Sci. Technol. **28**, 035011 (2013).
6. H. Richter, M. Wienold, L. Schrottke, K. Biermann, H. T. Grahn, and H.-W. Hübers, "4.7-THz local oscillator for the GREAT heterodyne spectrometer on SOFIA," IEEE Trans. Terahertz Sci. Technol. **5**, 539–545 (2015).
7. H.-W. Hübers, S. G. Pavlov, A. D. Semenov, R. Köhler, L. Mahler, A. Tredicucci, H. E. Beere, D. A. Ritchie, and E. H. Linfield, "Terahertz quantum cascade laser as local oscillator in a heterodyne receiver," Opt. Express **13**, 5890–5896 (2005).
8. H.-W. Hübers, R. Eichholz, S. G. Pavlov, and H. Richter, "High resolution terahertz spectroscopy with quantum cascade lasers," J. Infrared Millim. Terahertz Waves **34**, 325–341 (2013).
9. Q. Qin, B. S. Williams, S. Kumar, J. L. Reno, and Q. Hu, "Tuning a terahertz wire laser," Nat. Photon. **3**, 732–737 (2009).
10. M. S. Vitiello and A. Tredicucci, "Tunable Emission in THz Quantum Cascade Lasers," IEEE Trans. Terahertz Sci. Technol. **1**, 76–84 (2011).
11. D. Turčinková, M. I. Amanti, F. Castellano, M. Beck, and J. Faist, "Continuous tuning of terahertz distributed feedback quantum cascade laser by gas condensation and dielectric deposition," Appl. Phys. Lett. **102**, 181113 (2013).

#291900 https://doi.org/10.1364/OE.25.016282
Journal © 2017 Received 31 Mar 2017; revised 12 May 2017; accepted 18 May 2017; published 29 Jun 2017

Optics EXPRESS

12. M. Wienold, B. Röben, L. Schrottke, and H. T. Grahn, "Evidence for frequency comb emission from a Fabry-Pérot terahertz quantum-cascade laser," Opt. Express **22**, 30410–30424 (2014).
13. K. Ohtani, M. Beck, and J. Faist, "Electrical laser frequency tuning by three terminal terahertz quantum cascade lasers," Appl. Phys. Lett. **104**, 011107 (2014).
14. N. Han, A. de Geofroy, D. P. Burghoff, C. W. I. Chan, A. W. M. Lee, J. L. Reno, and Q. Hu, "Broadband all-electronically tunable MEMS terahertz quantum cascade lasers," Opt. Lett. **39**, 3480–3483 (2014).
15. D. Turčinková, M. I. Amanti, G. Scalari, M. Beck, and J. Faist, "Electrically tunable terahertz quantum cascade lasers based on a two-sections interdigitated distributed feedback cavity," Appl. Phys. Lett. **106**, 131107 (2015).
16. F. Castellano, V. Bianchi, L. Li, J. Zhu, A. Tredicucci, E. H. Linfield, A. G. Davies, and M. S. Vitiello, "Tuning a microcavity-coupled terahertz laser," Appl. Phys. Lett. **107**, 261108 (2015).
17. M. Hempel, B. Röben, L. Schrottke, H.-W. Hübers, and H. T. Grahn, "Fast continuous tuning of terahertz quantum-cascade lasers by rear-facet illumination," Appl. Phys. Lett. **108**, 191106 (2016).
18. L. Diehl, C. Pflügl, M. F. Witinski, P. Wang, T. J. Tague, and F. Capasso, "Fourier transform spectrometers utilizing mid-infrared quantum cascade lasers," in "CLEO/QELS: 2010 Laser Science to Photonic Applications," (2010), pp. 1–2.
19. R. Eichholz, H. Richter, S. G. Pavlov, M. Wienold, L. Schrottke, R. Hey, H. T. Grahn, and H.-W. Hübers, "Multi-channel terahertz grating spectrometer with quantum-cascade laser and microbolometer array," Appl. Phys. Lett. **99**, 141112 (2011).
20. P. Dean, M. Salih, S. P. Khanna, L. H. Li, N. K. Saat, A. Valavanis, A. Burnett, J. E. Cunningham, A. G. Davies, and E. H. Linfield, "Resonant-phonon depopulation terahertz quantum cascade lasers and their application in spectroscopic imaging," Semicond. Sci. Technol. **27**, 094004 (2012).
21. D. Burghoff, T.-Y. Kao, N. Han, C. W. I. Chan, X. Cai, Y. Yang, D. J. Hayton, J.-R. Gao, J. L. Reno, and Q. Hu, "Terahertz laser frequency combs," Nat. Photon. **8**, 462–467 (2014).
22. M. Rösch, G. Scalari, M. Beck, and J. Faist, "Octave-spanning semiconductor laser," Nat. Photon. **9**, 42–47 (2014).
23. Y. Yang, D. Burghoff, D. J. Hayton, J.-R. Gao, J. L. Reno, and Q. Hu, "Terahertz multiheterodyne spectroscopy using laser frequency combs," Optica **3**, 499 (2016).
24. D. Burghoff, Y. Yang, and Q. Hu, "Computational multiheterodyne spectroscopy," Sci. Adv. **2**, e1601227 (2016).
25. L. Schrottke, X. Lü, G. Rozas, K. Biermann, and H. T. Grahn, "Terahertz GaAs/AlAs quantum-cascade lasers," Appl. Phys. Lett. **108**, 102102 (2016).
26. L. S. Rothman, I. E. Gordon, Y. Babikov, A. Barbe, D. C. Benner, P. Bernath, M. Birk, L. Bizzocchi, V. Boudon, L. R. Brown, A. Campargue, K. Chance, E. A. Cohen, L. H. Coudert, V. M. Devi, B. J. Drouin, A. Fayt, J.-M. Flaud, R. R. Gamache, J. J. Harrison, J.-M. Hartmann, C. Hill, J. T. Hodges, D. Jacquemart, A. Jolly, J. Lamouroux, R. J. L. Roy, G. Li, D. A. Long, O. M. Lyulin, C. J. Mackie, S. T. Massie, S. Mikhailenko, H. S. P. Müller, O. V. Naumenko, A. V. Nikitin, J. Orphal, V. Perevalov, A. Perrin, E. R. Polovtseva, C. Richard, M. A. H. Smith, E. Starikova, K. Sung, S. Tashkun, J. Tennyson, G. C. Toon, V. G. Tyuterev, and G. Wagner, "The HITRAN2012 molecular spectroscopic database," J. Quant. Spectrosc. Radiat. Transfer **130**, 4–50 (2013).
27. S. Kumar, B. S. Williams, Q. Qin, A. W. M. Lee, Q. Hu, and J. L. Reno, "Surface-emitting distributed feedback terahertz quantum-cascade lasers in metal-metal waveguides," Opt. Express **15**, 113–128 (2007).
28. H. Richter, M. Greiner-Bär, S. G. Pavlov, A. D. Semenov, M. Wienold, L. Schrottke, M. Giehler, R. Hey, H. T. Grahn, and H.-W. Hübers, "A compact, continuous-wave terahertz source based on a quantum-cascade laser and a miniature cryocooler," Opt. Express **18**, 10177–10187 (2010).
29. A. Yariv, *Optical Electronics* (Saunders College, 1991), 4th ed.
30. L. A. Dunbar, R. Houdré, G. Scalari, L. Sirigu, M. Giovannini, and J. Faist, "Small optical volume terahertz emitting microdisk quantum cascade lasers," Appl. Phys. Lett. **90**, 141114 (2007).
31. H. Zhang, G. Scalari, J. Faist, L. A. Dunbar, and R. Houdré, "Design and fabrication technology for high performance electrical pumped terahertz photonic crystal band edge lasers with complete photonic band gap," J. Appl. Phys. **108**, 093104 (2010).

1. Introduction

Many spectroscopic techniques rely on a powerful radiation source with a wide spectral coverage. In the technologically underdeveloped terahertz (THz) frequency range, which corresponds to important transitions in atoms, molecules, and solids, quantum-cascade lasers (QCLs) are promising sources for diverse spectroscopic applications due to their high emission powers.

Unprecedented resolution and sensitivity has been achieved due to the narrow linewidth of single-mode THz QCLs in continuous-wave (cw) operation. In order to obtain the spectrum of a gas absorption line, the laser mode can be continuously tuned over the line, which leads to a corresponding variation of the detector signal [1–3]. A QCL can also be employed to obtain the spectrum of, for example, black body radiation transmitted through a gas cell or of THz radiation from outer space [4–6]. For this purpose, the QCL acts as a local oscillator in a heterodyne

Optics EXPRESS

detection scheme, in which the original spectrum is converted down to radio frequencies and then investigated by a spectrum analyzer [4–8].

The achievable continuous coverage of these techniques is limited by the low intrinsic tuning range of THz QCLs in cw operation, which is usually below 5 GHz. Many techniques have been developed to increase the continuous tuning range, but it is either extended only moderately or the increase comes at the cost of high complexity, low emission power, low tuning speeds, or insufficient reproducibility [9–17].

For the spectroscopy of absorption lines of gases and absorption bands of long molecules such as explosives, multi-mode QCLs have also been employed in the mid-infrared and THz spectral range [18–20]. In the case of the THz QCLs, a frequency range of 100 to 300 GHz was covered. However, the obtained spectra exhibit gaps of more than 20 GHz, since the low tuning range also persists for multi-mode QCLs. While spectral gaps on this order might be acceptable for the spectroscopy of slowly varying absorption bands, they prevent the application of THz QCLs as sources for versatile high-resolution spectroscopy. Frequency combs based on multi-mode THz QCLs [12, 21–24] may also generate a spectrum with a continuous coverage over a certain frequency range, but the spectral coverage typically also contains gaps.

In this work, we demonstrate that a multi-mode THz QCL can be employed as a high-power replacement for conventional THz wideband sources used in Fourier transform infrared spectroscopy. We achieve a gapless coverage over a range of 72 GHz at about 4.7 THz using a principle which we will refer to as gapless time-averaged wideband (G-TAWB) operation. We will analyze the emission spectrum of the QCL in G-TAWB operation and demonstrate its superiority to conventional sources in terms of signal-to-noise ratio, dynamic range, and reproducibility of the transmission spectra. Since G-TAWB operation is based on a QCL that is strongly tunable by a fast ramp of the injection current, we also discuss the tuning mechanism and compare the performance of several similar QCLs.

2. Principle and setup

The employed multi-mode QCL is based on a Fabry-Pérot (FP) resonator. Figure 1(a) shows a sketch of a typical FP spectrum, which consists of several equally spaced modes. The spectral positions of the FP modes ν_M are given by

$$\nu_M = \frac{cM}{2L_{\mathrm{opt}}}\,, \tag{1}$$

where $L_{\mathrm{opt}} = nL$ is the optical path length determined from the refractive index of the waveguide mode n and the length L of the resonator. The order of the FP mode M represents the number of intensity maxima of the standing wave in the resonator and amounts to at least 100 for typical resonator lengths. c denotes the speed of light in vacuum. Altering L_{opt} by a small amount dL_{opt} changes the frequency of a FP mode by

$$d\nu_M = -\frac{cM}{2L_{\mathrm{opt}}^2} dL_{\mathrm{opt}}\,. \tag{2}$$

Neighboring FP modes shift practically by the same amount, since $d\nu_{M+1} \approx d\nu_M$ for large M. If the collective shift exceeds the mode spacing as indicated in Figs. 1(b) and 1(c), the overall continuously covered frequency range is the product of the mode spacing and the number of active modes, which approaches the total width of the gain profile.

Using this quasi-continuous tuning scheme, a QCL can in principle be adjusted such that one laser mode operates at any desired emission frequency within the operating range. However, in contrast to conventional wideband sources for spectrometers, the QCL cannot emit a continuous spectrum at one point in time. In order to use the QCL as a high-power replacement for conventional spectrometer sources, the QCL must be tuned in a short time interval Δt, while the

Optics EXPRESS

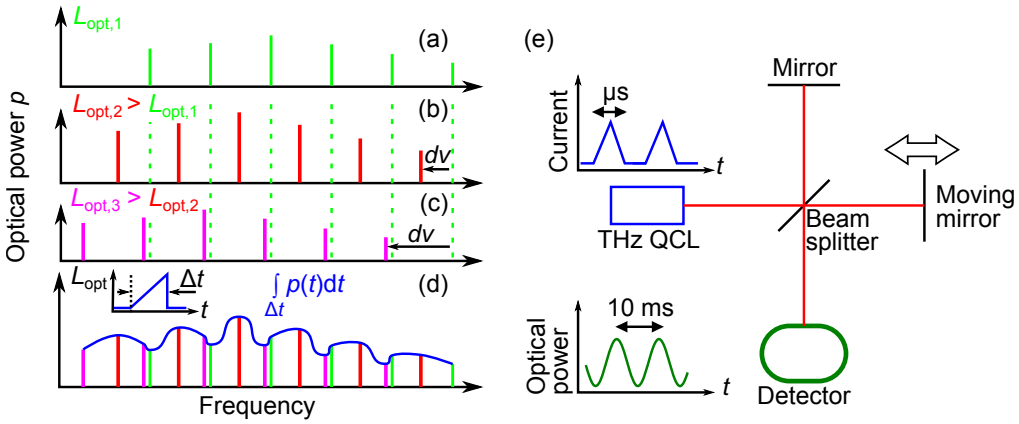

Fig. 1. (a)–(c) Schematic emission spectra of QCLs with FP resonators for increasing optical path lengths L_{opt}. The modes in (b) and (c) are collectively red-shifted by an amount $d\nu$, which can be larger than the mode spacing as shown in (c). (d) If the optical path length is continuously increased over a time Δt and the spectral power p is averaged over this time span, a wide, gapless spectrum may be generated, which is referred to as G-TAWB operation. (e) Setup for a Fourier transform infrared spectrometer with a THz QCL under G-TAWB operation.

signal of the spectrometer detector is averaged over this time span, as sketched in Fig. 1(d). If Δt is substantially smaller than the acquisition time of the spectrometer, the emission spectrum appears to be continuous due to the averaging so that we obtain G-TAWB operation.

The main challenge to realize G-TAWB operation is to tune the discrete FP modes over a frequency range which closes the spectral gaps between these modes. For about 3-mm-long FP resonators, which are typical for pulsed-mode operation of THZ QCLs, we observe mode spacings of about 10 GHz. The typically achievable current-induced tuning for this kind of devices in pulsed operation is below 10 GHz for many of our QCLs. However, some QCLs exceed a tuning range of 10 GHz, from which we select the most suitable one to demonstrate G-TAWB operation. A discussion of the tuning mechanism and a comparison of several QCLs is given in section 4.

Figure 1(e) depicts the experimental setup using a THz QCL in G-TAWB operation as a source for a Fourier transform infrared (FTIR) spectrometer. The employed GaAs/AlAs QCL was fabricated from the same wafer as the QCL with the lower doping density in [25]. The QCL with a single-plasmon waveguide has a width of 120 μm and a length of about 3 mm. The QCL is mounted on the cold finger of a continuous-flow cryostat operated at 10 K, which is placed in front of the external emission port of the spectrometer. The volume between the exit window of the cryostat and the entrance window of the evacuated spectrometer is purged with nitrogen to reduce absorption by water vapor in air. In order to realize the current ramp for G-TAWB operation, we employ an ILX Lightwave LDP-3840 pulsed driver with a pulse width set to 1 μs and triggered at 300 kHz. Using a smoothening capacitor, the original rectangular pulse can be transformed into a triangular one, yielding a current ramp amplitude of about 1 A and a maximum voltage of about 8 V.

The time-averaging is realized by employing a slow pyroelectic detector [deuterated triglycine sulfate (DTGS)] for the spectrometer, which does not follow the fast intensity changes due to the current ramp. The detector has its highest sensitivity for intensity variations between 10 and 100 Hz, which corresponds to the typical frequencies of the intensity variation due to the continuously moving mirror of the interferometer. The highest resolution of the employed

spectrometer (Bruker IFS 120HR) is 0.105 GHz (0.0035 cm^{-1}). To compare the performance of the THz QCL in G-TAWB operation with a conventional source, a heated SiC rod, also known as a *globar*, is employed, which is part of the spectrometer and therefore optimized to its optics and running at full capacity.

3. QCL in G-TAWB operation as a spectrometer source

Figure 2(a) shows the emission spectrum of the QCL in G-TAWB operation recorded with the highest resolution of the spectrometer. The measurement parameters, including the aperture, have been chosen in such a way that any broadening effects are minimized. We observe a continuous coverage of 72 GHz over the range from 4.686 to 4.758 THz. We confirmed that the gapless spectrum is not due to artifacts by investigating the tuning of the modes for rectangular current pulses at different current amplitudes. The spectrum is not smooth, since not only the position of the FP modes, but also their power and number are a function of the injection current. This is also the reason why only part of the 200-GHz-wide emission spectrum displayed in the inset of Fig. 2(a) shows a gapless coverage.

Figure 2(b) shows the emission spectra of the QCL in G-TAWB operation and of the high-performance thermal source based on a heated SiC rod, which is delivered with the FTIR spectrometer, with a lower resolution than in Fig. 2(a). In comparison to the thermal source, the QCL exhibits one to two orders of magnitude higher powers. The spectrum of the thermal source is not smooth due to its low power, which is on the order of the detector noise. Note that the hatched rectangle in Fig. 2(b) marks a peak which we attribute to a pickup of the power line frequency in the detector circuitry, through which an additional signal is introduced into

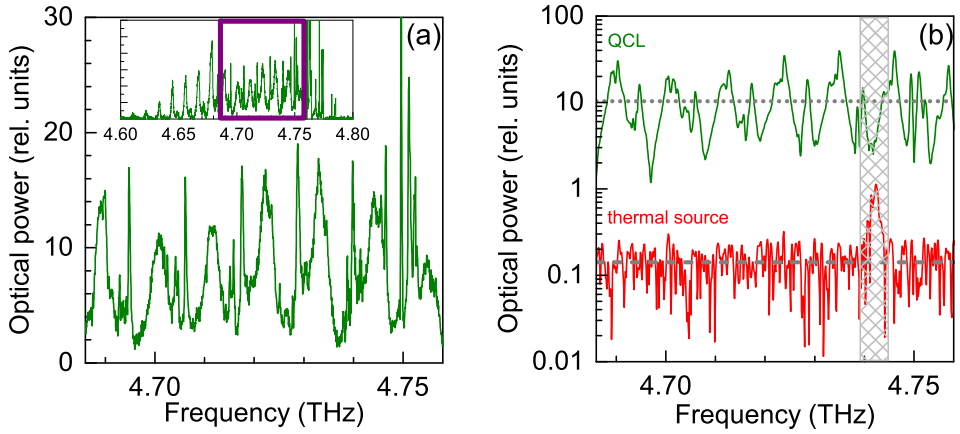

Fig. 2. (a) Spectral power in relative units of the QCL in G-TAWB operation for a frequency range of 72 GHz (4.686 to 4.758 THz). In order to investigate the continuity of the emission spectrum, the highest possible resolution was chosen, which amounts to 0.105 GHz (0.0035 cm^{-1}). To minimize any broadening effects in the spectrum, the Boxcar apodization, the Mertz phase correction, and an aperture of 8 mm are employed. The scanner speed is set to 10 kHz. Inset: Overview of the whole emission spectrum between 4.6 and 4.8 THz. The rectangle shows the gapless range of the spectrum. (b) Spectral power of the thermal source compared with the QCL in G-TAWB operation as measured with an FTIR spectrometer using a spectral resolution of 0.3 GHz (0.01 cm^{-1}) and the same aperture as well as scanner speed as in (a). The hatched rectangle marks a peak due to an electronic pickup and is therefore neglected in the analysis. The dotted and dashed lines mark the average power of 10.4 for the QCL and 0.14 for the thermal source, respectively.

Optics EXPRESS

the interferogram. The peak in the spectrum shifts to another position outside the investigated spectral region if for example a scanner speed of 7.5 instead of 10 kHz is selected. This peak can therefore be neglected in the analysis.

An important criterion of a spectroscopic system is its signal-to-noise ratio (SNR), which is a measure for the ability to discern a weak signal from noise. It can be determined from several consecutively recorded spectra taken under the same conditions, from which then, for every point in frequency, the mean is divided by the standard deviation. Figure 3(a) shows the SNR of the QCL and the thermal source calculated from 10 consecutive measurements. As in Fig. 2(b), the changing SNR over the frequency stems, in case of the QCL, from its varying power, and, in case of the thermal source, from its low output power comparable to the detector noise. Over the complete frequency range, the SNR of the QCL is significantly higher than the SNR of the thermal source. However, the SNR of the QCL as compared to the thermal source is not as large as one may have expected from a comparison of the emission spectra. While the average powers in Fig. 2(b) differ by a factor of about 75, the average SNR of the QCL is only a factor of about 20 higher than the average SNR of the thermal source. Since the measurements have been performed with the same spectrometer settings and detector, this difference must result from the noise of the QCL. More specifically, the emission spectrum of the QCL fluctuates in time, which is most likely due to a variation in the current pulses, which can be reduced by using a highly stable voltage-to-current converter. Note that the effect of the electronic pickup is only visible for the thermal source, since the QCL has a much higher emission power.

Apart from the SNR, the dynamic range is another important parameter for a spectroscopic system. To calculate the dynamic range, the detector noise level must be determined while the radiation from the emission source is blocked. The dynamic range can then be calculated by dividing the emission spectrum by the measured noise level. It is therefore a measure of the maximal absorption which can be distinguished from noise. To determine the noise level of the employed detector, the radiation source was blocked at the entrance aperture of the sample compartment using aluminum foil, whose low thermal emissivity ensures that no additional thermal radiation impinges on the detector. The noise level obtained by recording spectra in

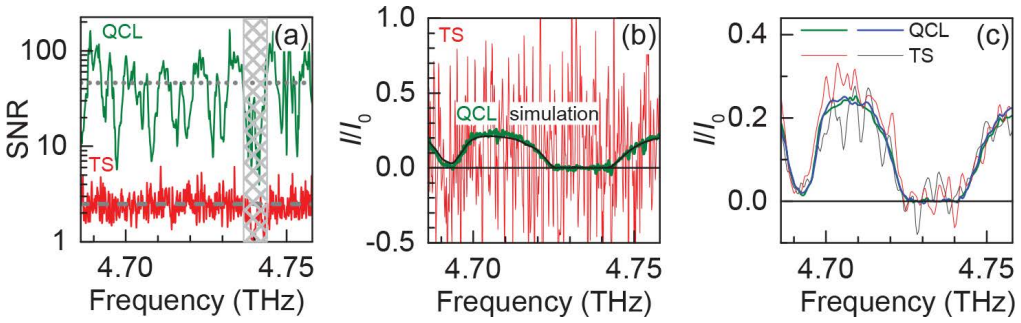

Fig. 3. (a) Signal-to-noise ratio (SNR) as a function of frequency. The dotted and dashed lines mark the average SNR of 46 for the QCL and 2.5 for the thermal source (TS), respectively. The hatched rectangle is explained in the caption Fig. 2(b). (b) Transmission spectrum of air with 100% humidity in a 10-cm-long gas cell recorded with the TS and with the QCL in G-TAWB operation. The resolution is set to 0.3 GHz (0.01 cm^{-1}), the scanner speed to 7.5 kHz, and the aperture to 8 mm. The acquisition time amounts to 143 s. The black curve displays a simulated transmission spectrum. (c) Transmission spectrum of the same gas cell as in (b), but recorded with different parameters. The resolution is set to 1.5 GHz (0.05 cm^{-1}), the scanner speed to 2.2 kHz, and the aperture to 12.5 mm. In order to investigate the reproducibility, two measurements employing both, the QCL and the TS, are displayed.

Optics EXPRESS

this configuration amounts to 0.04 relative units. Since the QCL power varies between 2 and 30 relative units according to Fig. 2(b), the resulting dynamic range is between 50 and 750. The thermal source, in contrast, has a power of about 0.14 relative units, leading to a dynamic range of only 3.5.

A characteristic property of the emission spectrum of the QCL in G-TAWB operation as compared to the spectrum of the thermal source is its strongly varying emission power as a function of frequency. In order to show that this variation does not hamper the reliability of a measurement, we recorded a transmission spectrum of a 10-cm-long gas cell filled with water-saturated air at atmospheric pressure, since it is expected to be slowly varying due to the strong pressure broadening of the water absorption lines. The absence of narrow peaks in the transmission spectrum may then prove that the structured emission spectrum does not prevent an accurate measurement. To demonstrate the superiority of the QCL as a spectrometer source, we compare the results using the QCL and the thermal source. Figure 3(b) shows the transmission spectra of air with 100% humidity in a 10-cm-long gas cell taken with the QCL in G-TAWB operation and with the thermal source. The transmission spectrum was obtained by dividing a spectrum with the gas cell positioned in the sample chamber of the spectrometer by a subsequently taken spectrum without the cell. Figure 3(b) also shows a simulated spectrum obtained from the HITRAN database based on the *model tropics, USA,* at 296 K [26]. While the measurement employing the QCL as a source clearly shows the slowly varying transmission spectrum in agreement with the simulated spectrum, the emission power of the thermal source is too low for a meaningful measurement. Note that the peak due to an electronic pickup, which is marked by a hatched rectangle in Figs. 2(b) and 3(a), has shifted out of the investigated frequency range due to the different scanner speed. In order to confirm the validity of the obtained results, we repeated the measurements with a reduced noise level by decreasing the resolution from 0.3 to 1.5 GHz and the mirror speed from 7.5 to 2.2 kHz. Figure 3(c) shows the resulting transmission spectra. To investigate the reproducibility, both measurements with the QCL and with the thermal source were repeated. In contrast to the measurement at higher resolutions, the spectra recorded using the thermal source now show reasonable results. However, the comparison of the nominally identical spectra and the presence of negative values between 4.73 and 4.74 THz reveal that the quickly varying modulation in the spectra of the thermal source is due to noise. In contrast, the transmission spectra using the QCL as a source are smooth and well-reproducible despite the strongly varying power in the emission spectrum.

4. Tuning mechanism and investigation of additional QCLs

The G-TAWB operation relies on the strong current-induced tuning of a THz QCL. There are two established mechanisms in the literature, which may explain the strong tuning of our QCL. First, the frequency of the laser mode can be tuned by changing the waveguide/resonator temperature, by which the refractive index of the material is modified [27]. The temperature change can either be realized by directly changing the temperature of the cryostat cold finger or by changing the injection current of the QCL in cw or high-duty-cycle pulsed operation, through which the produced heat is altered [8, 28]. The temperature change is a relatively slow process, which occurs on time scales exceeding 10 μs [17]. The achievable tuning range is determined by the functional dependence between material refractive index and temperature as well as by the temperature range where the QCL operates. Since improving these factors is difficult, the typical tuning range of THz QCLs based on single-plasmon waveguides is limited to several GHz.

A second tuning mechanism is the modification of the active-region refractive index by frequency pulling [29–31]. A different optical gain (or loss) always leads to a modification of the refractive index, since both values are coupled by the Kramers-Kronig relations. In contrast to the tuning by temperature, this is a very fast process as it is coupled to the gain build-up in the THz QCL. Therefore, this mechanism is compatible with the fast tuning at 300 kHz observed for

Optics EXPRESS

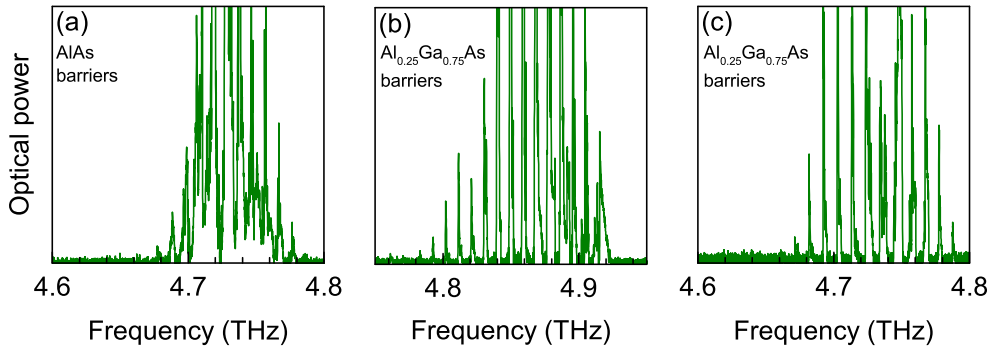

Fig. 4. Emission spectra of three additional THz QCLs for TAWB operation with (a) AlAs barriers such as the QCL considered so far as well as (b) and (c) $Al_{0.25}Ga_{0.75}As$ barriers. The QCLs used for (b) and (c) are similar to the ones presented in [5].

the QCL in G-TAWB operation. Since the gain profile and its dependence on the current can vary significantly even for similar heterostructure designs, the achievable tuning range is also expected to differ.

Figure 4 shows emission spectra of three additional QCLs in TAWB operation, which are similar in terms of their wavefunction structure, center frequency, and waveguide/resonator dimensions to the QCL considered so far in this work. Figure 4(a) displays the spectrum of a GaAs/AlAs QCL, where the miniband width has been increased and the coupling to the injection level improved compared to the GaAs/AlAs QCL discussed so far. For TAWB operation, the spectrum is narrower than for the GaAs/AlAs QCL shown in the inset of Fig. 2(a), but still exhibits an almost continuous coverage over a frequency range of 60 GHz with a narrow gap at 4.7240 THz. Figures 4(b) and 4(c) display the spectra of two additional QCLs with $Al_{0.25}Ga_{0.75}As$ barriers, which are almost identical in their design with sample B2 in [5]. The QCLs exhibit a maximal tuning of the individual modes of 7.5 and 6.6 GHz, respectively, which does not span the mode spacing of about 10 GHz. While all QCLs exhibit a tuning range well above 5 GHz, only the QCLs based on AlAs barriers exhibit sufficient tuning in order to close the spectral gaps between the FP modes. Apparently, the reduced leakage currents due to the higher barriers also have a significant impact on the current-dependent gain profile in addition to the improved wall-plug efficiency demonstrated in [25]. A more detailed investigation to identify the influence of AlAs barriers for the increased tuning range is beyond the scope of this paper.

5. Conclusion

We have shown that a THz QCL in G-TAWB operation can create an emission spectrum without spectral gaps over a frequency range of 72 GHz, which can be used as a source for Fourier transform infrared spectroscopy. Due to the high emission powers of THz QCLs, they are superior to commonly used wideband sources for spectroscopy in terms of SNR and dynamic range by a factor of 10 to 100. An advantage of the presented technique using a multi-mode QCL in G-TAWB operation is that the modes have only to be tuned by a fraction of the total emission bandwidth in contrast to tunable single-mode QCLs. A second advantage of this method is the absolute frequency scale of the spectrum obtained by the FTIR spectrometer without the necessity of calibrating the tuning characteristics of the QCL. The properties of the presented QCLs in G-TAWB operation can be optimized in several respects with regard to their application in spectroscopy. First, a QCL with an active region designed for a larger spectral range, which is known to be possible up to a bandwidth exceeding 1.7 THz [22], would clearly

Optics EXPRESS

be very useful for high-resolution and wideband THz spectroscopy. A better understanding of the mechanism responsible for the large current-induced tuning observed in some QCLs is necessary in order to design future active regions for a maximized tuning range. To provide alternative or complementary approaches, fast tuning mechanisms compatible with QCLs with FP resonators, such as for example the facet illumination with near-infrared light, should be also further improved [17]. Since QCL-related noise was found to reduce the SNR, employing a highly stable voltage-to-current converter to provide the current ramps promises a higher sensitivity. With this kind of current source, the spectrum of a QCL in G-TAWB operation may also be smoothed. This may be achieved by modified pulse shapes such as a set of ramps with different slopes to compensate for low emission powers at small currents. In summary, QCLs in G-TAWB operation pave the way for versatile high-sensitivity and high-resolution spectroscopy at THz frequencies.

Acknowledgments

We would like to thank W. Anders for sample processing, A. Tahraoui for fruitful discussions, and A. Hernández-Mínguez for a critical reading of the manuscript.